Increased Apoptosis of Host Cells and Tumor Cells in the Invasion Front of Colorectal Liver Metastases

OBUL REDDY BANDAPALLI*, NAWID HARIRI*, STEPHAN MACHER-GÖPPINGER, CHRISTOPH KAHLERT, PETER SCHIRMACHER and KARSTEN BRAND

Institute of Pathology, University Hospital Heidelberg, University of Heidelberg, 69120 Heidelberg, Germany

Abstract. *Background: The invasion front of colorectal liver metastases is an area of intensive tumor cell–host cell contact. Materials and Methods: In a xenograft nude mouse model, we analyzed whether apoptosis induction is a prominent feature in this active area, perhaps offering new modalities of therapeutic intervention. Results: Using global gene expression technology, an over-representation of apoptosis-related biological themes in the invasion front was observed. A combination of apoptosis-specific TUNEL/DAPI staining and cell type-specific staining showed that all examined cell types, including tumor cells, hepatocytes, endothelial cells, macrophages and hepatic stellate cells, displayed increased apoptosis in the invasion front. Evaluation of gene expression of the death receptor/ligand pairs TRAILR2 /TRAIL and FAS/FASL indicated that tumor cells overexpressed TRAILR2 and FAS, whereas host cells expressed TRAIL and FASL. Conclusion: This data indicates that the invasion front of colorectal liver metastases is an area of prominent pro-apoptotic activity, involving known death receptor/ligand interactions.*

Colorectal carcinoma is the second most frequent cancer disease in both sexes (1). For patients with this type of cancer, liver metastases are the main cause of death. They often remain the only manifestation of the disease once the primary tumor has been surgically removed (2-4). Besides standard treatment modalities such as surgical intervention and chemotherapy, a number of molecular-based approaches for the treatment of colorectal liver metastases have been examined during the last two decades (5).

*Both Authors contributed equally to this work.

Correspondence to: Karsten Brand, Institute of Pathology, University Hospital Heidelberg, University of Heidelberg, Im Neuenheimer Feld 220/1, D-69120 Heidelberg, Germany. Tel: +49 06221564057, Fax: +49 0622156 5251, e-mail: karsten.brand@med.uni-heidelberg.de

Key Words: Apoptosis, liver metastases, invasion front, FAS, TRAIL, colorectal cancer.

Apart from proliferation and invasiveness, resistance of tumor cells against apoptosis is a decisive parameter for successful tumor growth and metastasis. Since apoptosis is at least in part driven by ligand–receptor interactions, it has early been recognized that tumor cell–host cell interaction may play a crucial role in apoptosis induction. However, due to the current knowledge, host cells as well as tumor cells seem to operate as apoptosis inducers as well as recipients of pro-apoptotic signals. Whereas in some scenarios apoptosis induction in tumor cells by host cells is seen (6, 7), counter-attack mechanisms exerted by tumor cells killing invading inflammatory cells or even parenchymal cells are reported in other situations (8, 9).

A region which is particularly well suited to studying tumor-cell–host cell interaction is the invasion front of colorectal liver metastases, where tumor cells and host cells are in direct contact or communicate by paracrine signals.

To obtain a global overview of tumor cell–host cell interactions in the invasion front of colorectal liver metastases, we have studied murine models and clinical specimens using global gene expression profiling and functional studies (10-13). Utilizing a nude mouse model of colorectal liver metastasis (nude/LS174T), we have demonstrated a very pronounced host cell reaction on invading tumor cells comprising the biological themes of cell communication, cell adhesion, extracellular matrix production and many more (11). Likewise, tumor cells of the invasion front display a number of features that distinguish them from their counterparts in the tumor center. Using *ex vivo* and *in vivo* gene transfer technology, we were able to show that the invasion front is apparently a very vulnerable site amenable to therapeutic intervention, including the induction of apoptosis (14). The current study was undertaken to examine the degree of apoptotic activity in this respective animal model, irrespective of any therapeutic intervention, in order to provide a more comprehensive picture of apoptotic mechanisms in a native situation.

We found increased apoptosis in the tumor cells as well as in the host cells of the invasion front, as compared to central parts of the tumor or non-involved liver. Species-specific examination of expression levels of the well known

ligand–receptor pairs FAS/FASL and TRAILR/TRAIL suggest that the death ligands are mainly expressed by host cells to kill tumor cells that exhibit high expression of the respective receptors. This data indicates that the invasion front is an active area with respect to apoptosis and warrants further studies to elucidate underlying mechanisms.

Materials and Methods

Animal experiments. LS174T human colon adenocarcinoma cells were cultured in RPMI supplemented with 10% FCS, 2 mM glutamine, 100 IU/ml penicillin and 50 mg/ml streptomycin. Six to 10-week-old female athymic nude mice (NMRI-*nu/nu*; Möllegard und Bomholdgard Laboratorien, Ry, Denmark) were anesthetized using Ethomidat (Radenarkon; Asta Medica, Frankfurt, Germany) at a concentration of 40 μg/g body weight. They were subjected to a lateral abdominal incision extending just below the last left rib in a sickle shape of about 1 cm. The spleen was luxated and 50 μl of 5×10^6 LS174T cells were injected into the tip of the spleen using a 30.5 gauge needle. Alternatively, mice were subjected to a midline abdominal incision extending from the xiphoid process to just above the urinary bladder. A volume of 50 μl of 5×10^6 LS174T cells were injected along the margin of the large liver lobe. Both models produce extensive liver colonization after a period of 4-6 weeks. At that time, animals were euthanized, livers were removed and 10 mm-thick pieces containing tumor areas and liver were embedded in TissueTek OTC medium (Sakura, Tokyo, Japan), snap-frozen in methylbutane, pre-cooled in liquid nitrogen and stored at −80˚C.

Immunofluorescence and apoptosis double staining. Serial formalin-fixed tissue sections of LS174T-derived tumors were used for immunofluorescence and apoptosis double staining. Briefly, 1 μm sections were de-paraffinized with xylene and passaged through decreasing concentrations of ethanol. Subsequently, antigen retrieval was performed by heating the slides in 10 mM citric acid in a microwave oven (1×1 min, 750 W) at pH 6.0. After washing with 1× PBS (2×5 min), the tissue sections were incubated with polyclonal sheep anti mouse albumin (Acris antibodies, Hiddenhausen, Germany; 1:200, Cat no. NB120-8940), monoclonal mouse anti-human β-catenin (BD, Biosciences, Pharmingen, USA; 1:100, clone 14, Cat. no. 610154), monoclonal rat anti-mouse CD31 (BD Biosciences, Pharmingen; 1:100, clone MEC 13.3), monoclonal rat anti-mouse CD68 (Acris; 1:50, F4/80 antigen, clone A3-1) or polyclonal rabbit anti mouse desmin antibodies (Progen Biotechnik, Heidelberg, Germany; 1:50, Cat. no. 10570) at 4˚C overnight. After washing with 1× PBS for 3×5 min, they were incubated with secondary antibodies (anti-sheep/anti-mouse/anti-rat/anti-rabbit) conjugated with the green fluorescent stain Alexa 488 (MoBiTec, Göttingen, Germany) or for non histochemical staining using the Vectastain ABC Kit PK-4006 or PK-4006-4 (Vector Laboratories, Burlingame, CA, USA) for 30 min. After washing with 1× PBS for 3×5 min., for TUNEL staining the sections were incubated with 50 μl of TdT enzyme and fluorochrome mixture for 1 h at 37˚C in dark (*In Situ* Cell Death Detection Kit, TMR red (Roche Diagnostics, Mannheim, Germany). The sections were then washed with 1×PBS for 3×5 min. and then DAPI staining was performed (Roche) for 15 min at 37˚C in the dark. Then sections were washed two times with 1×PBS for 5 min each and fixed with fluoromount (SouthernBiotech, Birmingham, USA). The slides were analyzed under a fluorescence microscope.

Laser microdissection (LMD). Frozen tissue blocks were cut into 8-μm sections using a cryostat (Leica, Wetzlar, Germany) and stained using cresyl violet according to the Ambion LCM staining kit protocol (Austin, TX, USA). After microscopic examination of staining quality and tissue preservation, the sections were used for microdissection using either a Leica AS LMD (Leica, Wetzlar, Germany) or MMI (Molecular Machines and Industries, Eching, Germany). Four distinct cell populations were separately microdissected with LCM equipment a) pure liver tissue (L) at least 10 rows away from the invasion front, b) liver invasion front (LI) tissue extending 5 cell rows into the liver, c) tumor invasion front (TI) tissue extending 5 cell rows into the tumor and d) pure tumor tissue (T) at least 10 rows away from the invasion front.

RNA extraction of LCM samples. Total RNA was extracted from each sample of laser-microdissected tissue with the RNeasy Mini Kit (Qiagen, Hilden, Germany) according to the manufacturer's recommendations, including a DNase I digestion step and elution in 15 μl RNase-free water.

Reverse transcription (RT) of RNA and second-strand synthesis. RT was performed as previously described (15) with some modifications: 10 μl of the purified total RNA from RT was mixed with 2 μl dT_{24}-T_7-Primer (20 μM 5'-GGCCAGTGAATT GTAATACGACTCACTATAGGGAGGCGG-$(dT)_{24}$-3'; TibMolBiol, Berlin, Germany) to initiate first-strand synthesis. Primer and RNA were incubated for 5 min at 70˚C, followed by incubation for 2 min at 42˚C. Next, 4 μl of 5 × first-strand reaction buffer, 2 μl 0.1 M DTT, 1 μl 10 mM dNTPs, 1 μl 40 U/μl RNAsin (Promega, Mannheim, Germany) and 1 μl 200 U/μl Superscript II (Invitrogen, Karlsruhe, Germany) were added and incubated for 1 h at 42˚C. Next, 91 μl RNase-free water, 30 μl 5 × second-strand synthesis buffer, 3 μl 10 mM dNTPs, 1 μl 10 U/μl *Escherichia coli* ligase, 4 μl 10 U/μl DNA polymerase I and 1 μl 2 U/μl *E. coli* RNase H were added and the mixture was incubated for 2 h at 16˚C, followed by a 5-min incubation step at 16˚C after the addition of 2 μl 5 U/μl T4 DNA polymerase. The reaction was stopped by the addition of 10 μl of 0.5 M EDTA at pH 8. cDNA was extracted with phenol-chloroform and NH_4-acetate precipitation

RNA amplification. First-round T7-based RNA amplification was performed using the T7 Megascript Kit (Ambion, Huntingdon, U.K.): 12 μl cDNA were mixed at room temperature with 2 μl T7-buffer, 2 μl 40 mM NTPs and 2 μl enzyme mix and incubated for 9 h at 37˚C. The RNA was extracted with phenol-chloroform and NH4-acetate precipitation. The pellet was re-suspended in 10 μl RNase-free water.

For subsequent rounds of RNA amplification, a total of 10 μl of RNA from the first-round amplification was mixed together with 2 μl 50 ng/μl random hexamers (Invitrogen), incubated for 10 min at 70˚C, then chilled on ice and equilibrated at room temperature for 10 min. Then 4 μl 5 × first-strand buffer, 2 μl 0.1 M DTT, 1 μl 10 mM dNTPs, 1 μl 40 U/μl RNasin and 1 μl 200 U/μl Superscript II were added and incubated for 1 h at 37˚C. Subsequently, 1 μl RNase H was added and incubated at 37˚C for 20 min, after which the reaction mix was heated to 95˚C for 2 min and chilled on ice. For the second-strand synthesis, 1 μl T7-$(dT)_{24}$ primer was added and incubated at 70˚C for 5 min and at 42˚C for 10 min. Next, 92 μl RNase-free water, 30 μl 5 × second-strand buffer, 3 μl 10 mM dNTPs, 4 μl DNA polymerase I and 1 μl RNase H were added and

Table I. *Over-representation of apoptosis-related GO-terms in the liver invasion compartment as compared to the liver compartment (upper panel) and over-representation of apoptosis related GO-terms in the tumor invasion compartment as compared to the tumor compartment (lower panel).*

Over-represented in liver invasion compartment as compared to liver		
GO-Term	Name	Single test *p*-value
8629	Induction of apoptosis by intracellular signals	0.09
8630	DNA damage response, signal transduction resulting in induction of apoptosis	0.04
42771	DNA damage response, signal transduction by p53 class mediator resulting in induction of apoptosis	0.04
Over-represented in tumor invasion front as compared to tumor		
GO-Term	Name	
6919	Caspase activation	0.029
6927	Programmed cell death, transformed cells	0.076
8656	Caspase activator activity	0.0073
16505	Apoptotic proteases activator activity	0.018
42981	Regulation of apoptosis	0.08

incubated at 16˚C for 2 h; 2 μl T4 DNA polymerase were added and incubated at 16˚C for 10 min. The cleanup of the double-stranded cDNA was performed as described for the first round of amplification. cDNA was then ready for second-round T7 *in vitro* transcription and RT, which were performed as described for the first round. Then a third round of RNA amplification/labeling was performed as described in the next paragraph.

Biotinylated cRNA target was generated as previously described (16) from both amplified and non-amplified cDNAs using the Bioarray high-yield transcription kit (ENZO, New York, NY, USA) following the manufacturer's protocol. After a 5-h incubation period at 37˚C, the final biotin-labeled cRNA product was purified using RNeasy spin columns (Qiagen) and eluted twice in 30 μl of RNase-free water. The concentration of biotin-labeled cRNA was determined by UV absorbance. In all cases, 20 μg of each biotinylated cRNA preparation were fragmented, assessed by gel electrophoresis and placed in a hybridization cocktail containing 4 biotinylated hybridization controls (BioB, BioC, BioD and Cre) as recommended by the manufacturer.

Microarray hybridization and data analysis. Labeled samples were hybridized for 16 h either with murine MOE430 A&B or Human HGU U133A&B (Affymetrix, Santa Clara, CA, USA) GeneChip arrays. Arrays were washed and stained according to the instrument's standard Eukaryotic GE Wash 2' protocol using antibody-mediated signal amplification. The scanned images from the chips were processed using Affymetrix Microarray GCOS software, Microarray Database software, Excel (Microsoft, Seattle, WA) and GOSSIP (Microdiscovery, Berlin, Germany).

Semiquantitative qPCR. Microdissection for relative qPCR was essentially performed as for hybridization experiments. Total RNA of microdissected liver and liver invasion was isolated as described for hybridization experiments. Quantitative PCR experiments were performed with a real-time PCR detection system (Roche), using LightCycler RNA Master SYBR Green I mix and LightCycler 480 DNA SYBR Green I master (Roche). Specific primers for respective genes were designed using primer3 software (Whitehead Institute, Cambridge, MA, USA) and verified for specificity by *in silico* PCR (http://genome.cse.ucsc.edu/cgi-bin/hgPcr). The sequences for *18S* RNA are forward primer 5'-AAACGGCTACCACATCCAAG-3', reverse primer 5'-CCTCCAATGGATCCTCGTTA-3', *FAS* forward primer 5'-TCAGTACGGAGTTGGGGAAG-3', reverse primer 5'-CAGGCCTTCCAAGTTCTGAG-3', for *FASL* forward primer 5'-GCCCATGAATTACCCATGTC-3', reverse primer 5'-GCCACAGA TTTGTGTTGTGG-3', for *TRAIL* forward primer 5'-TCAGCACTT CAGGATGATGG-3', reverse primer 5'-CTGCTTCATCTCG TTGGTGA-3', and for *TRAILR2* forward primer 5'-TGCAGCCG TAGTCTTGATTG-3', reverse primer 5'-TCCTGGACTTCCATTT CCTG-3'. Obtained raw values of crossing points for *FAS, FASL, TRAIL* and *TRAILR2* were normalized by 18S RNA values to correct for RNA quality. In addition, differences in PCR amplification efficiencies of 18S RNA and the genes under examination were accounted for by calculation of the respective efficiencies in serial two-fold dilutions of non-microdissected tissue RNA and normalization to the obtained ratio. The observed differences in crossing point analysis were transcribed into fold changes according to efficiency values.

Results

Global gene expression profiles reveal biological themes that argue for increased apoptosis in both tumor cells and host cells. We first wanted to obtain a global overview of potential apoptotic mechanisms involved in the invasion front of colorectal liver metastases. To this extent, four areas, namely liver further away from the invasion front, liver invasion, tumor invasion and tumor further away from the invasion front were defined as explained in the materials and methods section. Compartments were separately microdissected. RNA was isolated and hybridized on whole-genome gene expression chips (Affymetrix). Subsequently, over-representation of biological themes was determined by Gossip software (17). As displayed in Table I, a number of biological themes

representing apoptotic mechanisms were significantly over-expressed in the liver part of the invasion front as compared to the liver further away from the invasion front, as well as in the tumor part of the invasion front as compared to the central parts of the tumor. Due to the dual species nature of our animal model and hybridization on murine or alternatively on human chips, we were able to distinguish genes expressed by host cells (murine origin) and tumor cells (human origin). Accordingly, in Table I the comparison of TI/T only includes human genes and thus represents a comparison of tumor cells (human origin) in the respective compartments only. Likewise, the comparison LI/L only compares host cells (murine origin). Thus, we conclude that host cells, as well as tumor cells of the invasion front, as compared to the respective non-invasion front cells overexpress genes involved in apoptosis.

Increased apoptosis in the liver part and the tumor part of the invasion front as compared to the inner parts of the tumor or the liver. On the basis of the gene expression studies described above, we hypothesized that increased expression of pro-apoptotic genes would correspond to increased apoptosis of the involved cells. We therefore determined the number of apoptotic cells in the different compartments by a combination of detection of DNA strand breaks (TUNEL) and morphologic assessment by DNA staining (DAPI) (Figure 3A). The invasion front compartments displayed a 10-fold (LI) or a 7-fold (TI) higher number of apoptotic cells per area than the respective central compartments (L, T, Figure 1A) indicating that the invasion front is indeed a region of increased apoptosis.

Determination of cell types displaying increased apoptosis in the invasion front. We next investigated, which cell types contribute to the observed increase of apoptosis. To this and, we combined apoptosis-specific staining (TUNEL/DAPI) with cell type-specific staining of tumor cells and resident host cells. Tumor cells were detected with beta-catenin staining, which is highly expressed by LS174 cells (10), whereas more typical antigens such as CK20 or CK19 are not expressed by this undifferentiated colorectal cancer cell line (data not shown). Murine hepatocytes were detected with albumin staining, hepatic stellate cells (HSCs) with desmin staining (Figure 3B), endothelial cells with CD31 staining, and macrophages with CD68 staining. All examined cell types displayed more apoptosis in the invasion front compartments than in the central parts (Figure 1B). As displayed in Figure 2A, most apoptotic cells in LI were hepatocytes and most apoptotic cells in TI were tumor cells. However, if the fraction of apoptotic cells of one particular cell type was compared to the whole number of this cell type (Figure 2B), endothelial cells seem to be most vulnerable to apoptosis in LI (Figure 2B). Taken together, this data indicates that all resident host cell types and tumor cells experience increased apoptosis in the invasion front, however, at different degrees of susceptibility.

Expression of FASL/FAS and TRAILR/TRAIL pairs in the invasion front compartments. To examine potential underlying mechanisms for increased apoptosis, we determined the expression of the well known pro-apoptotic ligand/receptor pairs TRAIL/TRAILR2 and FAS/FASL.

According to the microarray data, FAS was present on chips detecting gene products of human origin in the invasion front and tumor compartments but absent from the liver compartment and it was entirely absent from the chips detecting gene products of murine origin, indicating that FAS is expressed by tumor cells only (Table IIA). To confirm and to quantify this finding, we performed semi-quantitative qPCR utilizing human-specific primers (Table IIB). Tumor cell-derived human FAS was 7.8-fold higher in the tumor cells of the invasion front than in the center of the tumor.

In contrast, FASL was present on chips detecting gene products of murine origin in the liver invasion front, the tumor invasion front and the tumor compartment but absent in the liver compartment and it was entirely absent on the chips detecting gene products of human origin, indicating that FAS is expressed by murine cells only (Table IIA). Semi-quantitative qPCR (Table IIB) revealed that host cell-derived human FASL was 6.4-fold higher in the cells of the liver invasion front than in the center of the liver. The data indicate that FASL is exclusively expressed by hos-derived cells other than hepatocytes, including host cells invading the tumor.

Similar gene expression data was obtained for the TRAILR2/TRAIL pair. According to the chip data, TRAILR2 was present on chips detecting gene products of human origin in the invasion front compartment but was absent from the liver and tumor compartments and it was entirely absent from the chips detecting gene products of murine origin, indicating that FAS is expressed by invading tumor cells only (Table IIA). Semi-quantitative qPCR (Table IIB) revealed that expression of tumor cell-derived human TRAILR2 was 10.5-fold higher in the tumor cells of the invasion front than in the center of the tumor.

In contrast, TRAIL was present on chips detecting gene products of murine origin in all compartments except the tumor compartment and it was entirely absent from the chips detecting gene products of human origin, indicating that FAS is expressed by murine cells only (Table IIA). Semi-quantitative qPCR (Table IIB) revealed that expression of host cell-derived murine TRAIL was 14.5-fold higher in the cells of the liver invasion front than in the center of the liver. This data indicates that FASL is exclusively expressed by host derived cells.

This combination of species- and compartment-specific gene expression data suggests a predominant expression of death receptor ligands by host cells and of the respective death receptors by tumor cells. It also suggests that both death receptor ligands are highly expressed by host cells of the invasion front in order to kill tumor cells of the invasion front which express particularly high levels of the respective death receptors.

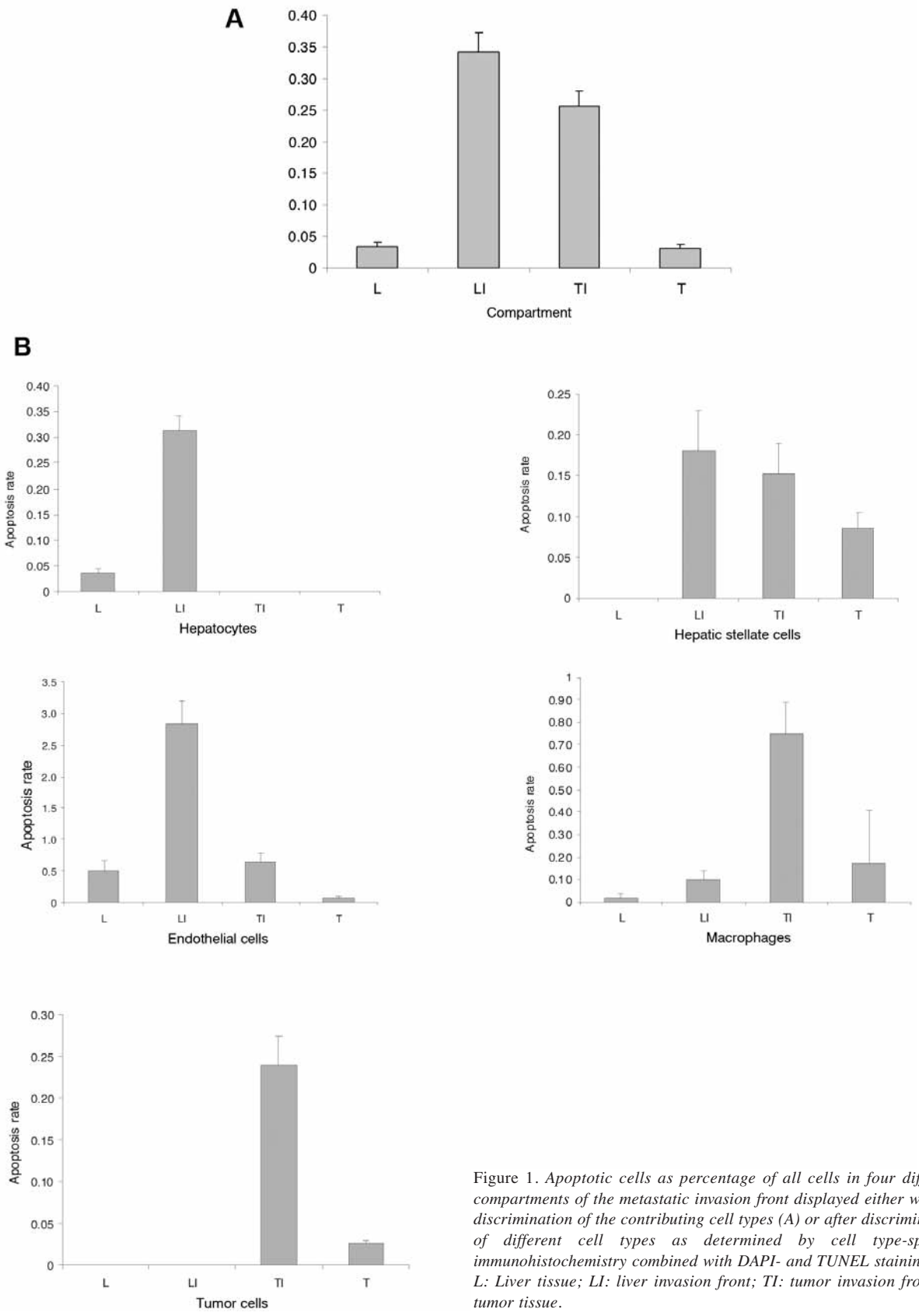

Figure 1. *Apoptotic cells as percentage of all cells in four different compartments of the metastatic invasion front displayed either without discrimination of the contributing cell types (A) or after discrimination of different cell types as determined by cell type-specific immunohistochemistry combined with DAPI- and TUNEL staining (B). L: Liver tissue; LI: liver invasion front; TI: tumor invasion front; T: tumor tissue*.

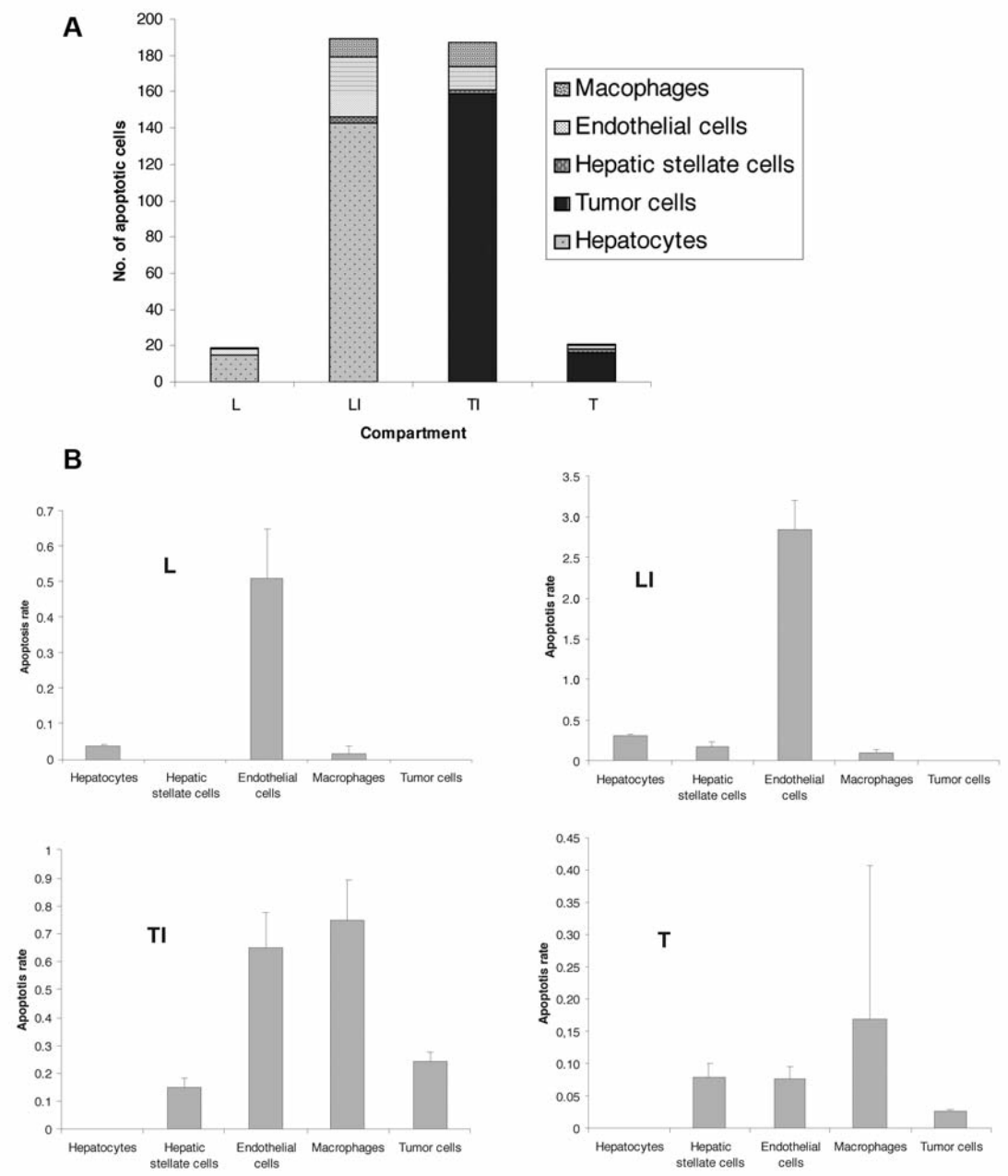

Figure 2. *A, B: Contribution of distinct cell types to apoptosis in different compartments, expressed either as absolute number of apoptotic cells of one distinct cell type (A) or as apoptotic cells of one distinct cell type as percentage of all counted cells of this cell type (cell type specific apoptosis rate, B).*

Discussion

This study examined cell type-specific apoptosis and possible underlying mechanisms in the invasion front of colorectal liver metastases. Increased apoptosis of all examined host cell types, as well as of tumor cells of the invasion front, was observed. Although to our knowledge a global *in vivo* analysis of apoptosis at the tumor-host interface has not been performed before, some reports have dealt with several aspects of this subject. The observed increased apoptosis of tumor cells of the invasion front as compared to tumor cells of the inner part of the tumor is probably the outcome of defensive mechanisms of the host. In a rat model of colorectal liver metastases, a sequential order of events was made responsible for tumor cell elimination, starting with a synergistic action of macrophages and NK cells (18), followed by pro-apoptotic

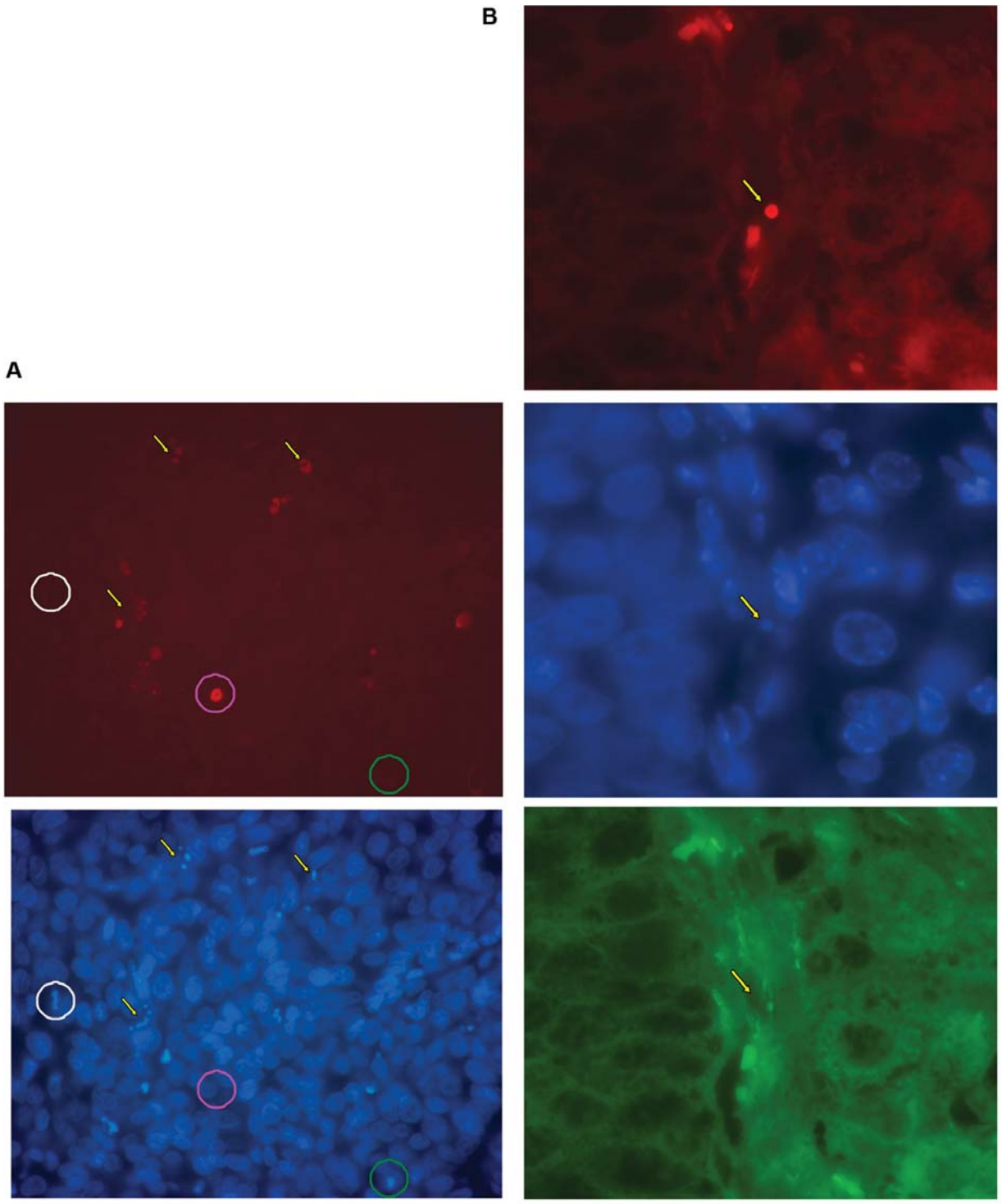

Figure 3. *Detection of apoptosis in the invasion front by double and triple fluorescence. A: Double staining is required for specific detection of apoptotic cells (red: TUNNEL; blue: DAPI): The white circle indicates a mitotic cell with the typical morphology seen with DAPI staining and as expected without a positive signal in TUNEL. The pink circle indicates a false-positive result in the TUNEL because no apoptotic nucleus is seen in DAPI despite there being a strong signal in TUNEL. The green circle marks a cell that could be interpreted as apoptosis if only DAPI staining is used, but the lack of positive TUNEL finding raises significant concern regarding this interpretation (false-positive in DAPI). In contrast, yellow arrows mark unequivocally apoptotic cells that are positive for TUNEL and DAPI. B: Triple fluorescence to detect hepatic stellate cell undergoing apoptosis: TUNEL (red) and DAPI (blue) indicate apoptosis as explained in A. Hepatic stellate cells are decorated by cytoplasmic and membranous green fluorescence due to staining with an anti-desmin antibody and a secondary antibody coupled to Alexa 488.*

Table II. *A, B: Expression of pro-apoptotic gene/receptor pairs. Expression of FAS/FASL and TRAILR2/TRAIL in different compartments was examined by hybridisation on murine or human Affymetrix microarrays (A) and the difference of expression levels between L and LI or T and TI (fold change) were determined by semi-quantitative PCR (B). A=absent call, P=present call.*

A	Murine					Human			
Gene	ID	L	LI	TI	T	ID	L	LI/TI	T
FAS	1460251_at	A	A	A	A	202535_at	A	P	P
FASL	1449235_at	A	P	P	P	210865_at	A	A	A
TRAILR2	1421296_at	A	A	A	A	209294_x_at	A	P	A
TRAIL	1420412_at	P	P	P	A	202688_at	A	A	A

B	Murine			Human	
		L	LI	TI	T
FAS				7.8 ←	
FASL		→	6.4		
TRAILR2				10.5 ←	
TRAIL		→	14.5		

effects of EC on tumor cells (19) and finally by cellular and immune defense systems, such as those offered by cytotoxic T-cells, monocyte-derived macrophages and others (20). Using clinical specimens of colorectal liver metastases, apoptosis of tumor cells was observed also (9).

With respect to apoptosis of host cells in clinical specimens and in the above mentioned rat model, a dramatically increased apoptosis of peritumoral hepatocytes as compared to tumor cells, and increased apoptosis of mononuclear cells, were reported (9, 21). In our model, these effects were less dramatic because the fraction of apoptotic hepatocytes as compared to all hepatocytes in the invasion front was just comparable to the fraction of apoptotic tumor cells. These results may indicate that counterattack mechanisms exerted by the invading tumor may be of less relevance in our animal model. In our model, among the examined host cells, hepatocytes comprise the dominant fraction of apoptotic cells, which is probably due to their mere numeric abundance as compared to the other host cell types. From the point of view of a growing tumor, apoptosis of hepatocytes makes sense because these parenchymal cells are probably of no particular use for the tumor stroma, or at least are not routinely observed within a tumor deposit and apparently just occupy space that is needed for invading tumor cells. Different from hepatocytes, the other examined host cell types all play a positive role in metastasis formation. Therefore, the interpretation of the meaning of increased apoptosis of these cells in the invasion front is not straight forward. The growing tumor is actually dependent on successful angiogenesis, and therefore increased apoptosis of endothelial cells in the invasion front is not intuitive. Interestingly, endothelial cells in our model were the cell type displaying the highest susceptibility for apoptosis. In a rat model of colorectal carcinoma, it was reported that hepatic endothelial cells and tumor cells kill each other by FAS/FASL- mediated apoptosis, apparently in a context-dependent fashion (20). However, the meaning of increased endothelial cell-apoptosis can only be speculated upon. Depending on the growth pattern of metastasis, a more or less dramatic reorganization of the liver structure is required (22). Thus, some endothelial cells, although principally needed, may not be at the right point at the right time and thus would need to be eliminated. Alternatively, these phenomena may be side-effects of a pro-apoptotic microenvironment at the invasion front leading to unwanted (from the viewpoint of the tumor) endothelial cell apoptosis. Similarly to endothelial cells, HSCs are probably predomiantly tumor promoting and the observed increased apoptosis is again not intuitive. HSCs produce a number of pro-fibrogenic molecules and appear to be responsible for the formation of a fibrotic capsule around the liver metastases (11). As such they have been looked at as being a defensive device of the tumor against invading and attacking inflammatory cells. In addition, they aid angiogenesis and are recruited into the tumor stroma (22, 23). In the liver, HSCs are probably the precursors of carcinoma-associated fibroblasts, which are known to have a tumor-supporting function (24-27). In accordance with this, a promotion of liver metastasis by HSCs has recently been reported (28). Altogether, increased apoptosis of HSCs in the

invasion front compartment may have similar reasons as assumed for endothelial cells, but a final explanation is still lacking. Finally, liver macrophages (Kupffer cells) constitute an effective first line of defense for the liver as they constantly face and eliminate foreign materials, bacteria, harmful chemicals as well as invading tumor cells (18, 29). They are capable of destroying malignant cells through phagocytosis, secretion of cytotoxic and cytostatic agents and interaction and communication with other immune cells *via* numerous cytokines. However, their tumoricidal function is limited and when metastases are established, they may even assist tumor growth and invasion, rather than hinder it *e.g.* by production of growth factors, cytokines and matrix metalloproteinases (29). Under these circumstances, the increase in apoptosis of macrophages that we observed may be tumor-promoting or tumor-preventive depending on the spatial and temporal context.

Which are the molecules involved in cell killing? We arbitrarily analyzed two well-known ligand/receptor pairs, TRAIL/TRAILR2 and FASL/FAS. We found TRAIL to be mainly expressed by the host cells of the liver invasion front and TRAILR2 by the tumor cells of the tumor invasion front. This finding, together with the observed dramatic increase of tumor cell apoptosis in the invasion front, argues for a preferential induction of apoptosis in invading tumor cells by defensive host cells by this receptor–ligand pair. This is in agreement with the well-known pro-apoptotic effect of TRAIL on tumor cells *in vitro* and *in vivo* including colorectal cancer and including clinical trials (30-32). Regarding tumor cell–host cell interaction in the liver, TRAIL-dependent tumor cell killing by resident liver cells, namely by NK cells, has been reported in a model of experimental liver metastases using a fibrosarcoma cell line (6). Nude mice, although deficient in T-cells, harbor NK cells in the liver such that tumor cell apoptosis in our model could, at least in part, be explained by this mechanism. According to our data, it is unlikely that the TRAIL–TRAILR interaction is responsible for increased host cell apoptosis in the invasion front as well, because TRAIL is not expressed on tumor cells and TRAILR2 is not expressed on host cells. Such a tumor counterattack mechanism has however been described for TRAIL/TRAILR, although the number of respective reports is more limited (33, 34) as compared to the FASL/FAS pair as described below.

With respect to the FASL/FAS pair, we found FAS to be overexpressed in the tumor cells of the invasion front. Since host tissue expressed FASL but not FAS, this death ligand-receptor interaction may account for tumor cell apoptosis in the invasion front in our model. This result is in agreement with the early reports obtained in diverse mouse xenograft tumors exhibiting antitumor effects upon activation of FAS (7, 35, 36) and more recent reports of apoptosis of FAS-expressing CC531 carcinoma cells by FASL expressing hepatic endothelial cells (19). However, particularly in colorectal cancer metastatic to the liver, the predominantly pro-apoptotic effect of FAS on tumor cells has been questioned (8). It has for example been reported that colorectal tumor cells, despite expressing FAS, are often resistant to FAS-mediated apoptosis (37) and a majority (6/8) of colon carcinoma cell lines co-express FAS and FASL without undergoing FAS-mediated apoptosis (38). However, our results indicate that this ligand/receptor pair may be effective in out model. Alternatively, in the literature the role of FASL expressed by tumor cells as a mechanism for counterattack against FAS-expressing host cells including inflammatory cells and hepatocytes (9) became more and more evident (8, 39). In one study, FASL was detected on tumor cells of the invasive margin of colorectal liver metastases from clinical specimen and FAS-expressing peritumoral hepatocytes showed increased apoptosis (9). Although we observed increased hepatocellular apoptosis in our murine model as well, the lack of FAS expression on hepatocytes and of FASL on tumor cells indicates that another mechanism seems to cause host cell apoptosis in our model. Further studies to evaluate in particular the mechanisms of host cell apoptosis are warranted because any resistance of host cells to pro-apoptotic signals might have prominent antitumor effects.

Acknowledgements

This study was financially supported by the European Union Framework Program 6; Grant number: LSHC-CT-2003-503297 to KB and the Young Investigator Award of the Medical Faculty, University of Heidelberg to ORB.

References

1 Becker N and Wahrendorf J: Krebsatlas der Bundesrepublik Deutschland. Springer, Berlin, 1997.
2 Dreben JA and Niederhuber JE: Cancer of the lower gastrointestinal tract. *In*: Current Therapy in Oncology. Niederhuber JE (ed.). Decker, St. Louis, MO, USA, pp. 426-431, 1993.
3 Grem JL: Current treatment approaches in colorectal cancer. Semin Oncol *18*: 17-26, 1991.
4 Curley SA, Izzo F, Abdalla E and Vauthey JN: Surgical treatment of colorectal cancer metastasis. Cancer Metastasis Rev *23*: 165-182, 2004.
5 Arnold D and Seufferlein T: Targeted treatments in colorectal cancer: state of the art and future perspectives. Gut *59*: 838-858, 2010.
6 Takeda K, Hayakawa Y, Smyth MJ, Kayagaki N, Yamaguchi N, Kakuta S, Iwakura Y, Yagita H and Okumura K: Involvement of tumor necrosis factor-related apoptosis-inducing ligand in surveillance of tumor metastasis by liver natural killer cells. Nat Med *7*: 94-100, 2001
7 Trauth BC, Klas C, Peters AM, Matzku S, Moller P, Falk W, Debatin KM and Krammer PH: Monoclonal antibody-mediated tumor regression by induction of apoptosis. Science *245*: 301-305, 1989.

8 O'Connell J, Bennett MW, Nally K, Houston A, O'Sullivan GC and Shanahan F: Altered mechanisms of apoptosis in colon cancer: Fas resistance and counterattack in the tumor-immune conflict. Ann NY Acad Sci *910*: 178-192; discussion 193-175, 2000.
9 Yoong KF, Afford SC, Randhawa S, Hubscher SG and Adams DH: FAS/FAS ligand interaction in human colorectal hepatic metastases: A mechanism of hepatocyte destruction to facilitate local tumor invasion. Am J Pathol *154*: 693-703, 1999.
10 Bandapalli OR, Dihlmann S, Helwa R, Macher-Goeppinger S, Weitz J, Schirmacher P and Brand K: Transcriptional activation of the beta-catenin gene at the invasion front of colorectal liver metastases. J Pathol *218*: 370-379, 2009.
11 Bandapalli OR, Geheeb M, Kobelt D, Kuehnle K, Elezkurtaj S, Herrmann J, Gressner AM, Weiskirchen R, Beule D, Bluthgen N, Herzel H, Franke C and Brand K: Global analysis of host tissue gene expression in the invasive front of colorectal liver metastases. Int J Cancer *118*: 74-89, 2006.
12 Bandapalli OR, Kahlert C, Hellstern V, Galindo L, Schirmacher P, Weitz J and Brand K: Cross-species comparison of biological themes and underlying genes on a global gene expression scale in a mouse model of colorectal liver metastasis and in clinical specimens. BMC Genomics *9*: 448, 2008.
13 Kahlert C, Bandapalli OR, Schirmacher P, Weitz J and Brand K: Invasion front-specific overexpression of tissue inhibitor of metalloproteinase-1 in liver metastases from colorectal cancer. Anticancer Res *28*: 1459-1465, 2008.
14 Brand K, Baker AH, Perez-Canto A, Possling A, Sacharjat M, Geheeb M and Arnold W: Treatment of colorectal liver metastases by adenoviral transfer of tissue inhibitor of metalloproteinases-2 into the liver tissue. Cancer Res *60*: 5723-5730, 2000.
15 Luo L, Salunga RC, Guo H, Bittner A, Joy KC, Galindo JE, Xiao H, Rogers KE, Wan JS, Jackson MR and Erlander MG: Gene expression profiles of laser-captured adjacent neuronal subtypes. Nat Med *5*: 117-122, 1999.
16 Luzzi V, Holtschlag V and Watson MA: Expression profiling of ductal carcinoma *in situ* by laser capture microdissection and high-density oligonucleotide arrays. Am J Pathol *158*: 2005-2010, 2001.
17 Bluthgen N, Brand K, Cajavec B, Swat M, Herzel H and Beule D: Biological profiling of gene groups utilizing gene ontology. Genome Inform *16*: 106-115, 2005.
18 Timmers M, Vekemans K, Vermijlen D, Asosingh K, Kuppen P, Bouwens L, Wisse E and Braet F: Interactions between rat colon carcinoma cells and Kupffer cells during the onset of hepatic metastasis. Int J Cancer *112*: 793-802, 2004.
19 Vekemans K, Braet F, Muyllaert D and Wisse E: Nitric oxide from rat liver sinusoidal endothelial cells induces apoptosis in IFN gamma-sensitized CC531s colon carcinoma cells. J Hepatol *41*: 11-18, 2004.
20 Braet F, Nagatsuma K, Saito M, Soon L, Wisse E and Matsuura T: The hepatic sinusoidal endothelial lining and colorectal liver metastases. World J Gastroenterol *13*: 821-825, 2007.
21 Vekemans K, Braet F and Wisse E: DiO-labeled CC531s colon carcinoma cells traverse the hepatic sinusoidal endothelium *via* the Fas/FasL pathway. J Gastrointest Surg *8*: 371-372; author reply 372, 2004.
22 Vermeulen PB, Colpaert C, Salgado R, Royers R, Hellemans H, Van Den Heuvel E, Goovaerts G, Dirix LY and Van Marck E: Liver metastases from colorectal adenocarcinomas grow in three patterns with different angiogenesis and desmoplasia. J Pathol *195*: 336-342, 2001.
23 Paku S, Kopper L and Nagy P: Development of the vasculature in 'pushing-type' liver metastases of an experimental colorectal cancer. Int J Cancer *115*: 893-902, 2005.
24 Bhowmick NA, Neilson EG and Moses HL: Stromal fibroblasts in cancer initiation and progression. Nature *432*: 332-337, 2004.
25 De Wever O and Mareel M: Role of tissue stroma in cancer cell invasion. J Pathol *200*: 429-447, 2003.
26 Mueller MM and Fusenig NE: Friends or foes – bipolar effects of the umour stroma in cancer. Nat Rev Cancer *4*: 839-849, 2004.
27 Kalluri R and Zeisberg M: Fibroblasts in cancer. Nat Rev Cancer *6*: 392-401, 2006.
28 Matsusue R, Kubo H, Hisamori S, Okoshi K, Takagi H, Hida K, Nakano K, Itami A, Kawada K, Nagayama S and Sakai Y: Hepatic stellate cells promote liver metastasis of colon cancer cells by the action of SDF-1/CXCR4 axis. Ann Surg Oncol *16*: 2645-2653, 2009.
29 Paschos KA, Majeed AW and Bird NC: Role of Kupffer cells in the outgrowth of colorectal cancer liver metastases. Hepatol Res *40*: 83-94, 2010.
30 Mahalingam D, Szegezdi E, Keane M, Jong S and Samali A: TRAIL receptor signalling and modulation: Are we on the right TRAIL? Cancer Treat Rev *35*: 280-288, 2009.
31 Falschlehner C, Ganten TM, Koschny R, Schaefer U and Walczak H: TRAIL and other TRAIL receptor agonists as novel cancer therapeutics. Adv Exp Med Biol *647*: 195-206, 2009.
32 Kruyt FA: TRAIL and cancer therapy. Cancer Lett *263*: 14-25, 2008.
33 Giovarelli M, Musiani P, Garotta G, Ebner R, Di Carlo E, Kim Y, Cappello P, Rigamonti L, Bernabei P, Novelli F, Modesti A, Coletti A, Ferrie AK, Lollini PL, Ruben S, Salcedo T and Forni G: A 'stealth effect': adenocarcinoma cells engineered to express TRAIL elude tumor-specific and allogeneic T-cell reactions. J Immunol *163*: 4886-4893, 1999.
34 Grimm M, Kim M, Rosenwald A, von Rahden B, Tsaur I, Meier, E, Heemann U, Germer CT, Gasser M and Waaga-Gasser AM: Tumour-mediated TRAIL-Receptor expression indicates effective apoptotic depletion of infiltrating $CD8^+$ immune cells in clinical colorectal cancer. Eur J Canc *46*: 2314-2323, 2010.
35 Coney LR, Daniel PT, Sanborn D, Dhein J, Debatin KM, Krammer PH and Zurawski VR Jr.: Apoptotic cell death induced by a mouse-human anti-APO-1 chimeric antibody leads to tumor regression. Int J Cancer *58*: 562-567, 1994.
36 Lucking-Famira KM, Daniel PT, Moller P, Krammer PH and Debatin KM: APO-1 (CD95)-mediated apoptosis in human T-ALL engrafted in SCID mice, Leukemia *8*: 1825-1833, 1994.
37 O'Connell J, O'Sullivan GC, Collins JK and Shanahan F: The Fas counterattack: Fas-mediated T-cell killing by colon cancer cells expressing Fas ligand. J Exp Med *184*: 1075-1082, 1996.
38 O'Connell J, Bennett MW, O'Sullivan GC, Roche D, Kelly J, Collins JK and Shanahan F: FAS ligand expression in primary colon adenocarcinomas: evidence that the FAS counterattack is a prevalent mechanism of immune evasion in human colon cancer. J Pathol *186*: 240-246, 1998.
39 Igney FH and Krammer PH: Immune escape of tumors: apoptosis resistance and tumor counterattack. J Leukoc Biol *71*: 907-920, 2002.

Received January 22, 2011
Revised March 4, 2011
Accepted March 8, 2011